Journal of Natural Gas Science and Engineering 34 (2016) 1276–1283

Contents lists available at ScienceDirect

Journal of Natural Gas Science and Engineering

journal homepage: www.elsevier.com/locate/jngse

Direct visualization of pore-scale fines migration and formation damage during low-salinity waterflooding

Wen Song, Anthony R. Kovscek*

Energy Resources Engineering, Stanford University, Stanford, CA, USA

ARTICLE INFO

Article history:
Received 30 March 2016
Received in revised form
8 July 2016
Accepted 23 July 2016
Available online 4 August 2016

Keywords:
Formation damage
Fines
Low-salinity waterflooding
Microfluidics
Flow visualization

ABSTRACT

Formation damage due to fines migration results, potentially, in significant decreases in reservoir permeability and, hence, the recoverability of crude oil from reservoirs. On the other hand, low salinity brine injection is a promising technique for increasing oil recovery from clay-rich sandstones in an economic manner. Clay detachment at low salinity conditions, however, drastically alters fluid flow. In this work, clay-functionalized etched-silicon micromodels are used to visualize directly the mobilization of clay at low salinity conditions in (i) the absence of oil, and (ii) the presence of oil. Study results include clay mobilization and pore plugging in the absence and presence of oil visualized by saturating the clay-functionalized micromodel with high salinity brine followed by injections of reduced salinity brines. Clay detachment and migration was observed in oil-free systems for 4000 ppm NaCl low salinity injection brine. The extent of fines detachment was quantified to determine the types of clay structures affected. Furthermore, fines migration, flocculation, and re-deposition were visualized directly. The types of structures formed (i.e., pore-plugging, pore-lining, etc.) by the re-deposited clay particles are characterized to determine their impact on formation damage. Clay detachment in the presence of oil was also visualized. Initial conditions analogous to clastic reservoirs were established by allowing the crude oil, brine, and solids to interact (i.e., age). Clay detachment occurred during 4000 ppm NaCl low salinity oil recovery. Real-time, pore-level visualization revealed significant mechanisms during oil recovery processes and their influence on multiphase flow. Specifically, pore plugging particles in water-filled pores obstructed preferential flow paths and diverted injection fluid to unswept regions thereby increasing oil production.

1. Introduction

Petroleum reservoirs often contain large quantities of both swelling and nonswelling clay (Khilar and Fogler, 1984; Kia et al., 1987; Mohan et al., 1993). Surface interactions between clay and its surroundings, i.e., brine, crude oil, and the bulk matrix significantly influence the petrophysical properties of the reservoir and the transport of fluids through the reservoir. Specifically, clays such as kaolinite and montmorillonite are prone to migration and swelling, respectively, as a result of contact with injection brines of altered compositions (Tang and Morrow, 1999; Schembre and Kovscek, 2004, 2005; Lager et al., 2008; Lever and Dawe, 1984). In reservoir engineering, formation damage, i.e., permeability reduction in the reservoir, is a key problem that arises during low salinity waterflooding (i.e., injection of brines with reduced salinity compared to the connate water or initial injection brine) in clay-rich sandstones (Khilar and Fogler, 1984; Mohan et al., 1993; Lemon et al., 2011; Hussain et al., 2014; Zeinijahromi et al., 2015).

Three main mechanisms have been proposed to explain reservoir formation damage under low salinity conditions: fines migration, particle swelling, and swelling-induced migration (Mohan et al., 1993). First, fines detachment and mobilization within the pore space may result in pore plugging phenomena that reduce the availability of flow paths. Specifically, the detachment and subsequent transport, flocculation, and redeposition of the free clay particles leads to significant pore-plugging, and ultimately formation damage. Kaolinite is particularly susceptible to this type of behavior under low salinity conditions. Second, clay swelling in the absence of stabilizing salt ions reduces the amount of pore space available to flow, and in severe cases of formation damage, blocks the smaller pore throats and hence reduces significantly the permeability of the reservoir. Montmorillonite is a smectite clay

* Corresponding author.
E-mail address: kovscek@stanford.edu (A.R. Kovscek).

http://dx.doi.org/10.1016/j.jngse.2016.07.055
1875-5100/

prone to swelling under low salinity conditions. Third, the swelling of pore-lining clays that subsequently break off fines during flow may lead to pore blockage and formation damage.

Low salinity brine injection, on the other hand, is a promising technique to increase oil recovery in clay-rich reservoirs. Specifically, Tang and Morrow (1999) first reported increases in oil recovery of an additional 5–20% of the original oil in place. Several mechanisms have been proposed to delineate the increase in oil recovery due to low salinity waterflooding, including fines migration, cation exchange, and emulsion formation. The effects of fines migration and possible formation damage on oil recovery, however, are not well understood. Disagreement in the literature and field-scale experiments suggests that fundamental understanding of the mechanisms dictating the low salinity effect is required (Mcguire et al., 2005; Boussour et al., 2009; Hadia et al., 2011; Skrettingland et al., 2011).

Pore-scale understanding of crude oil-brine-rock (COBR) behavior is critical to the optimal design of oil-recovery techniques with respect to formation damage. Core-flooding experiments have been conducted to study the fluid-fines interactions on clay detachment. Specifically, Khilar and Fogler (1984) studied the effect of injection brine salinity on overall fines migration and identified a critical salt concentration (CSC) that was required to mobilize kaolinite particles in Berea sandstone based on indirect pressure and effluent analysis. More recently, Hussain et al. (2014) performed both single- and two-phase low salinity waterflooding experiments in Berea sandstone cores to study the effect of fines migration on oil recovery. Specifically, significant permeability loss and slight increase in oil recovery were found. Core-scale experiments, however, are unable to resolve the fundamental formation damage mechanisms at the pore-scale. Current imaging technologies such as x-ray computed tomography cannot reach the spatial and temporal resolution that is required to visualize directly the in-situ, real-time pore-scale phenomena related to the behavior of the clay particles.

Microfluidics is an emerging technology that enables the direct visualization of pore-scale phenomena in real time (Buchgraber et al., 2012a, 2012b; Sinton, 2014). Recently, glass and silicon microfluidic devices with representative pore-scale geometries have enabled the study of petroleum fluid behavior in the subsurface (Buchgraber et al., 2012a, 2012b; Song and Kovscek, 2015; Song et al., 2014a,b). Specifically, Buchgraber et al. (2012a) described the creation of two-dimensional microfluidic platforms with etched geometries identical to those of real rock pores. These micromodels are unique microfluidic devices with the pore networks of real sandstones or carbonates etched into silicon and enable real-time, direct visualization of pore-scale phenomena that could not otherwise be observed in a core. Recently, Song and Kovscek (2015) incorporated clay particles within the micromodel to enable a visualization platform with both representative pore geometries and surface properties of real sandstone. These surface-functionalized micromodels incorporate the pore-scale surface heterogeneities that are associated with the presence of clays and enable the direct visualization of pore-level clay behavior such as clay sensitivity to injection brine composition, particle mobilization and swelling, and formation damage.

In this work, clay-functionalized micromodels were used to visualize directly the response of clay to low salinity brine injection. Montmorillonite and kaolinite clays were deposited onto the pore-wall surfaces of micromodels to enable the study of swelling and dispersive clays under low salinity conditions, respectively. Similarly, kaolinite and montmorillonite were deposited into the pore space to enable pore-scale study of crude oil/brine/rock interactions in a microfluidic platform with both realistic pore geometry and surface properties. Specifically, the effect of low salinity injection in rock rich in swelling clays (e.g., montmorillonite) and non-swelling clays (e.g., kaolinite) was studied through single-phase brine injection experiments, and the effect of fines migration and formation damage during low salinity oil recovery was studied through waterflooding experiments (i) the absence of oil, and (ii) the presence of oil. The extent of fines detachment was quantified to determine the types of clay structures affected. Structures formed (i.e., pore-plugging, pore-lining, etc.) by the re-deposited clay particles were characterized to determine their impact on formation damage. Clay detachment in the presence of oil was also visualized. Initial conditions analogous to clastic reservoirs were established by allowing the crude oil, brine, and solids to interact (i.e., age). Clay detachment occurred at roughly similar salinity. Real-time, pore-level visualization revealed significant mechanisms during oil recovery processes and their influence on multiphase flow. Specifically, pore plugging particles in water-filled pores obstructed preferential flow paths and diverted injection fluid to unswept regions thereby increasing oil production.

2. Experimental methods

Pore-scale visualization of formation damage in clay-rich sandstones due to low salinity waterflooding was achieved using surface-functionalized micromodels. The surface-functionalized micromodels are two-dimensional microfluidic visualization platforms with pore geometries and surface properties representative of those found in real reservoir rock. The micromodels consisted of a 5 cm × 5 cm porous matrix with a pore network etch depth of 30 μm to allow for pore-scale flow visualization. The porous matrix is constructed from repeating a base image of the sandstone geometry. Square areas of increasing widths were sampled and the associated porosities were calculated to determine the representative elementary volume (REV) of the system (see Supplementary Material). Specifically, the REV of the micromodel geometry here was determined to have a width of ~300 μm. The micromodel has a porosity of 54% and permeability of 2 Darcy.

The micromodels were fabricated in silicon and glass to achieve representative wettability properties of sandstone rock. Fabrication methods for the micromodel are as described by Buchgraber et al. (2012a) and Buchgraber et al. (2012b). Clay particles were deposited onto the pore walls to achieve representative surface wettability and structural properties of real reservoir rock. Kaolinite and montmorillonite were chosen to study the effect of low salinity injection on formation damage due to fines migration and swelling, respectively. The clay-functionalization of the micromodel pore surfaces in this work is similar to the methodology described in previously published work (Song and Kovscek, 2015). Specifically, a 1 wt% kaolinite solution was prepared by adding kaolinite powder (Kaolin, K2-500, Fisher Scientific) to 15,000 ppm NaCl (sodium chloride, S271-3, Fisher Scientific) solution and vigorously stirred at atmospheric conditions. The solution was sonicated (Bransonic 220) for 1 h before injection into the micromodel to prevent particle flocculation and pore plugging. The solution was then injected into the brine-saturated micromodel at 20 m/day to maintain particle dispersion and to minimize pressure buildup (Song and Kovscek, 2015). Montmorillonite was deposited into the micromodel in a similar fashion by injecting a solution with 1 wt% montmorillonite (Montmorillonite K 10, powder, CAS: 1318-93-0, Sigma-Aldrich) in 15,000 ppm NaCl into the brine-saturated micromodel to prevent swelling. Alternating air/brine injections were conducted to remove mobile clay particles; this ensured that the remaining clay particles were firmly adhered to the silicon surface. The clay-coated micromodel was continuously flushed with several pore volumes of the high salinity brine using the syringe pump to create a fully brine saturated system. The motivation

of saturating the micromodel with brine typical of a reservoir was two-fold: (1) to replicate the initial conditions in the reservoir, and (ii) to avoid clay detachment as a result of low salinity shock. All experiments were performed with constant injection rates and the micromodel outlets were maintained at atmospheric pressure.

2.1. Single phase montmorillonite experiments

Once sufficient montmorillonite was deposited onto the pore space, the surface-functionalized microfluidic network was flooded with 15,000 ppm NaCl solution to determine the initial single-phase permeability of the system. Specifically, the high salinity brine was injected at constant flow rate corresponding to a superficial velocity of 30 m/day using a 60 mL syringe (BD 60 mL syringe, 309653) and a syringe pump (Harvard Apparatus, Holliston, MA) setup, as shown in Fig. 1. The superficial velocity was determined using the injection flow rate, Q, and the cross sectional area, A, of the micromodel, i.e., $v = Q/A$. The system outlets were maintained at atmospheric pressure. Permeability was determined by measuring the pressure drop across the micromodel at constant injection rate. The micromodel was then imaged using a confocal microscope (Sensofar S neox 3D optical profiler) at 100 fixed locations across the micromodel to visualize the clay particle structure and distribution at initial conditions.

Formation damage due to clay swelling during low salinity brine injection was studied by flooding the system with deionized (DI) water to create a salinity shock. Pressure drop was measured across the micromodel to determine the impact of low salinity waterflooding on formation damage in the presence of swelling clays. The micromodel was imaged at the same locations to visualize any changes in the structure and distribution of the clay particles following the freshwater flood.

2.2. Single phase kaolinite experiments

Formation damage due to clay mobilization during low salinity brine injection was studied by flooding the kaolinite-functionalized micromodel with high and low salinity brines. Specifically, the micromodel was first saturated with high salinity brine (15,000 ppm NaCl) and imaged at 25 fixed locations across the micromodel to determine the initial clay distribution throughout the system. The basis for choosing the 25 locations was to create an evenly distributed grid of sampling locations throughout the micromodel. Specifically, the imaging grid formed 5 rows and 5 columns, each separated by 1 cm. We chose the origin to be at the bottom left corner of the 5 cm × 5 cm micromodel and coordinates of the first imaging location was ($x = 0.5$ cm, $y = 0.5$ cm). The 25 fixed pore locations were spaced evenly across the micromodel (i.e., a grid of 5 × 5 locations across the micromodel) to minimize the impact of pore-level heterogeneities. The selection process of the imaging locations was unbiased and thus allows for a more representative understanding of the pore-level behavior such as fluid saturations. Low salinity brine with 4000 ppm NaCl was injected into the micromodel to study the behavior of kaolinite under low salinity conditions. This salinity is below the critical salt concentration required to mobilize kaolinite in sandstone cores (Khilar and Fogler, 1984) and was thus chosen here. Images were taken at the same 25 fixed locations across the micromodel to determine the effect of low salinity brine injection on formation damage in the presence of dispersive clays.

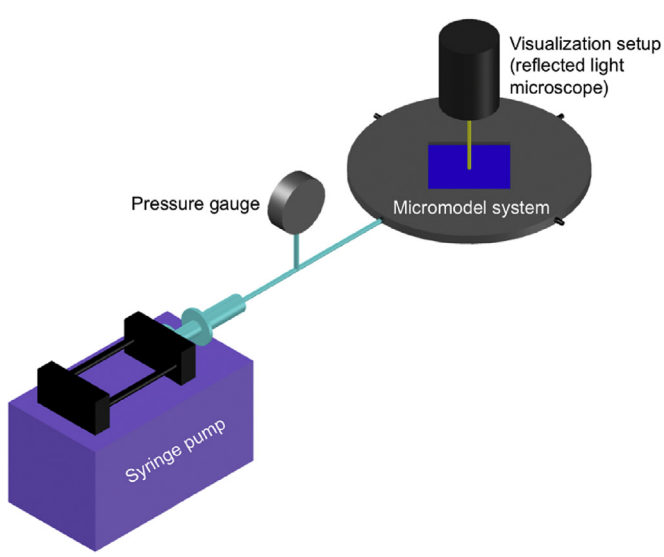

Fig. 1. Experimental setup for visualizing the mobility of clay particles within the micromodel. Saline solutions were injected using a syringe pump at a superficial velocity of 30 m/day. The microfluidic system was open to atmosphere downstream. Fluids and solids distributions were monitored throughout the duration of the flow experiments at a fixed location using the microscope-camera setup. The micromodel was imaged at a minimum of 25 fixed locations across the micromodel after each flow experiment to obtain spatial averages of the system response.

2.3. Two phase kaolinite experiments

Kaolinite was chosen to study oil recovery mechanisms in the presence of clay due to its prevalence in sandstone and the abundance of edge charges on the particle surface. The kaolinite-functionalized micromodel provided a two-dimensional visualization platform that was well representative of a real reservoir rock. Initial conditions representative of real reservoirs were required to conduct meaningful low salinity waterflooding experiments. In order to establish the initial conditions that were representative of clastic reservoir systems, the kaolinite-functionalized micromodel was saturated with formation brine and crude oil as follows. Table 1 lists the composition of the formation brine used. This is the formation brine composition that corresponds to the crude oil we chose to test.

The brine-saturated system was then imaged using confocal microscopy at 25 locations distributed evenly across the micromodel to determine the initial pore-scale clay distribution. The micromodel was then flooded with crude oil by injecting the crude oil at 30 m/day until residual water saturation was reached. The system was imaged during this process to observe the drainage process. The crude-oil properties are described in Table 2. This particular crude oil/brine system is of industrial relevance and was chosen here.

Low salinity experiments were conducted using crude oil due to the importance of surface interactions between kaolinite and the acid/base groups and asphaltenes in the crude oil. The micromodel was imaged immediately following the drainage process at the same 25 fixed locations to provide a basis for studying the effect of aging. The micromodel was aged for two weeks to allow for

Table 1
Composition of brine used to simulate initial conditions analogous to clastic reservoirs.

Reagent	Concentration (g/L)
$CaCl_2 \cdot 2H_2O$ (Calcium chloride dihydrate)	0.183
$MgCl_2 \cdot 6H_2O$ (Magnesium chloride hexahydrate)	0.585
NaCl (Sodium chloride)	20.461
KCl (Potassium chloride)	0.611
Na_2SO_4 (sodium sulfate)	0.109

Table 2
Crude oil characterization (Peng, 2009).

Crude oil properties	Value
Acid number (mg/g)	2.36
Base number (mg/g)	6.02
Asphaltene content (wt%)	2.69
Density (°API)	21

sufficient surface interactions between the various components in the crude oil, brine, clay, and silicon. Specifically, the system was submerged in a closed container of crude oil to avoid air from invading the pore space. The same 25 pore spaces were re-imaged after the aging process (i) to determine the effect that the interactions between the various phases had on the fluid distribution and wettability of the system and (ii) to obtain a pore-scale visualization of the initial condition.

After establishing the initial conditions that are representative of clastic reservoirs, the micromodel was subjected to a conventional high salinity waterflood. The high salinity waterflood was performed to serve as a benchmark against conventional oil recovery for subsequent flow experiments. Specifically, a 10,000 ppm brine was injected at a superficial velocity of 30 m/day for many pore volumes to benchmark the experiments against conventional waterflooding techniques. Pore-level saturations were directly visualized at the same 25 locations using confocal microscopy. To assess the effect of low salinity brine injection on the clay-functionalized micromodel system, a 4000 ppm low salinity brine was then injected. All experiments were conducted at ambient conditions with the outlets of the micromodels open to atmosphere.

2.4. Image processing

Images were processed to provide both quantitative and qualitative insight into the experimental results. Imaging at fixed locations across the micromodel allowed for visualization of fluid distribution evolution due to altered injection conditions. Specifically, images of fixed pore spaces were aligned to enable comparison of pore-level fluids/solids distributions between each stage of the flow experiments. Furthermore, images from two-phase experiments (i.e., waterflooding oil reservoirs) were binarized to distinguish between the various phases, i.e., crude oil, brine, and pore matrix. These image sequences provided (i) quantitative data on the saturations of the phases, and hence, oil recoveries after each injection process, and (ii) qualitative data on the pore-scale oil/brine distribution and preferential regions for clay and oil mobilization. All image processing was performed using Matlab and ImageJ.

3. Results and discussion

Kaolinite and montmorillonite particles were deposited into the microfluidic network to study directly the effect of low salinity brine injection on formation damage in clay-rich rock and its impact on oil recovery. The deposition techniques described by Song and Kovscek (2015) successfully achieved the representative fines structures, wettability properties, and salinity response resembling real sandstone. Specifically, montmorillonite particles were deposited as pore-lining particles and kaolinite particles exhibited both pore-lining and pore-plugging behavior. These deposition patterns correspond to the clay structures found in real sandstones. Second, wettability alteration of the micromodel due to the presence of clay was observed. Specifically, clay-dense pore-spaces were found to be non-wetting to the water phase in the presence of air. Third, a critical salt concentration (CSC between 4000 ppm NaCl and 6000 ppm NaCl) for kaolinite mobilization from the pore surface was identified and corresponds well to the literature for Berea sandstones. The clay deposition process was thus deemed valid to replicate rock properties within a micromodel and flow experiments were henceforth carried through to visualize directly the effect of low salinity fluids on the system.

3.1. Montmorillonite response to low salinity shock

Montmorillonite-functionalized micromodels were first saturated with a 15,000 ppm high salinity brine and subsequently flooded with a 4000 ppm low salinity brine. Pressure drop measurements across the clay-functionalized micromodel indicated significant formation damage due to the low salinity shock. Specifically, a 6-fold decrease in system permeability was measured from ~800 mD to ~130 mD. Alignment of the images at fixed locations before and after the low salinity waterflood allowed for direct monitoring of the effect of low salinity brine injection at the pore scale. Clay particle swelling was not visualized in this system, however significant fines migration was observed. Specifically, detachment of montmorillonite particles was highly sensitive to the injection brine salinity, as shown in Fig. 2 where the stably attached montmorillonite particles at high salinity (Fig. 2(a)) were released with the introduction of the low salinity brine (Fig. 2(b)). The visualization results here suggest that the dominant formation damage mechanism in the montmorillonite-rich micromodel was caused by swelling-induced fines migration, where clay swelling causes the detachment of other particles within the pore structure. Interestingly, low salinity core flooding experiments performed elsewhere (Mohan et al., 1993) concluded that swelling-induced fines migration contributed significantly to formation damage in montmorillonite-rich sandstones.

3.2. Kaolinite response to low salinity shock

Kaolinite-functionalized micromodels were initially saturated with a 15,000 ppm NaCl high salinity brine and subsequently subject to reduced salinity brine injections by order of decreasing salinity. Specifically, the single-phase brine injection experiments showed significant kaolinite mobilization at 4000 ppm NaCl. Fine clay particles were stably attached on the pore surface for injection brines from 15,000 ppm NaCl to 8000 ppm NaCl. Initial clay detachment was observed after 6000 ppm NaCl injection, and significant kaolinite mobilization was found for brine salinities at and below 4000 ppm NaCl. These results correspond well to experimental core data and theoretical particle stability calculations in the existing literature on the sensitivity of kaolinite mobilization to salinity (Schembre and Kovscek, 2005; Khilar and Fogler, 1984; Mohan et al., 1993).

Pore-level clay mobilization was quantified through image analysis of fixed pore spaces after each flow experiment. Regions affected by clay mobilization (e.g., detachment and redeposition) were recorded for each fixed pore location. Pore-scale images were obtained at each of the 25 fixed locations after high salinity (15,000 ppm NaCl) brine injection and low salinity (4000 ppm NaCl) brine injections were compared. Formation of pore-lining deposits and pore-bridging structures were observed. The regions affected by clay mobilization were aligned to the base image of the micromodel pore network. Summation of the images enabled characterization of the regions that were particularly susceptible to formation damage due to clay particle redeposition during low salinity waterflooding. Comparison between the formation damage map and single-phase flow simulation through the porous medium is shown in Fig. 3. Initial clay particle distributions within the pore

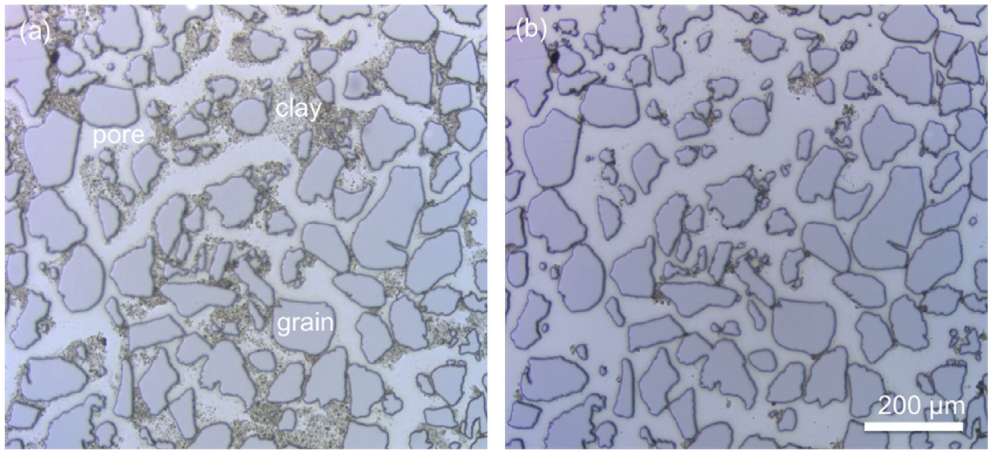

Fig. 2. Fines release and mobilization due to low salinity brine injection in a montmorillonite-rich sample. Initial clay particle distribution at 15000 ppm high salinity conditions (a) and mobilized montmorillonite distributions after the 4000 ppm low salinity waterflood (b) at the same pore location show significant fines release due to the low salinity shock.

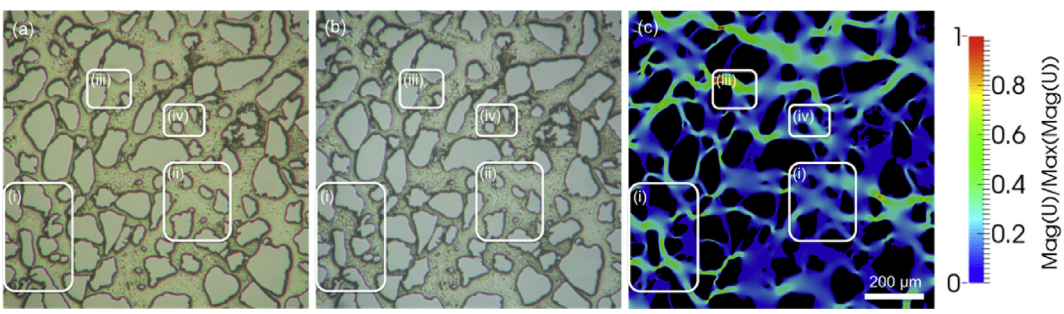

Fig. 3. Formation damage due to kaolinite mobilization during low salinity waterflooding. Initial clay particle distribution at 15000 ppm high salinity conditions (a) and mobilized kaolinite particles after 4000 ppm low salinity waterflooding (b) at the same pore location are compared with the single-phase velocity map from pore-scale simulation. Regions (i) and (ii) show the redepsotion of mobilized particles as pore-lining clays in the pores that were experiencing intermediate/slow velocities, while regions (iii) and (iv) show the formation of pore-bridging structures across high velocity flow paths. All simulated velocities shown in (c) are normalized against the maximum velocity of the porous system. Pore-scale simulations provided by Soulaine (2016).

space are shown in Fig. 3(a), while the effect of low salinity waterflooding is shown for the same pore space in Fig. 3(b). Fig. 3(c) shows the single-phase velocity map of the pore space obtained by solving the full Navier-Stokes equations for the micromodel pore geometry under the corresponding experimental conditions (Roman et al., 2015). All velocities shown in Fig. 3(c) are normalized against the maximum velocity of the simulation and thus vary from 0 (blue) to 1 (red). Furthermore, all velocities shown are consistent with the scale bar.

Formation damage due to clay mobilization was observed following the low salinity waterflood. Specifically, formation damage due to clay particle redeposition was most prevalently found in large pores that were experiencing flow of intermediate velocity (e.g., Fig. 3(i) and (ii)). Fig. 3(iii) and (iv) show that formation damage due to pore-bridging structures, however, were found to span small pores with high fluid velocity. While pore-bridging structures were not found at every pore with high fluid velocity, there was a higher probability of clay particles to form pore-bridging structures in those regions (i.e., the constrictions). These observations are consistent with current theories on pore-plugging mechanisms due to fines migration for non-swelling clays such as kaolinite (Mohan et al., 1993).

3.3. Oil recovery from kaolinite- and montmorillonite rich systems in response to low salinity shock

Two-phase experiments were conducted with kaolinite- and montmorillonite-functionalized micromodels, respectively. The system was saturated with the formation brine and subsequently injected with the corresponding crude oil. The system was aged at ambient conditions for two weeks to establish initial conditions representative of clastic reservoirs. Two weeks of aging allowed for sufficient interactions between the various components in the crude oil, brine, and solids and to reach thermodynamic equilibrium. No significant changes in the pore-level fluid behavior were observed for longer interaction time. Images were obtained at the 25 fixed locations across the micromodel after the aging process to establish the pore-level initial conditions.

Fig. 4 shows the direct visualization of the fluid distributions at a particular pore location near the center of the micromodel. Specifically, Fig. 4(a) shows the kaolinite-functionalized micromodel saturated with formation brine and Fig. 4(b) shows the initial condition at the same pore location. To understand the impact of low salinity waterflooding experiments and formation damage on the system, an initial 10,000 ppm high salinity waterflood was performed to provide a basis for comparison with conventional waterflooding results. The result of the high salinity brine injection is shown in Fig. 4(c). Next, a 4000 ppm low salinity brine was injected to investigate the effect of low salinity waterflooding on the system. The result of the low salinity brine injection is shown in Fig. 4(d). Oil was collected at the outlets of the microfluidic system, corresponding to a decrease in oil saturation throughout the micromodel and thus an increase in oil recovery.

Overall clay mobilization in the oil-brine system was difficult to quantify due to the relative opacity of the crude oil combined with

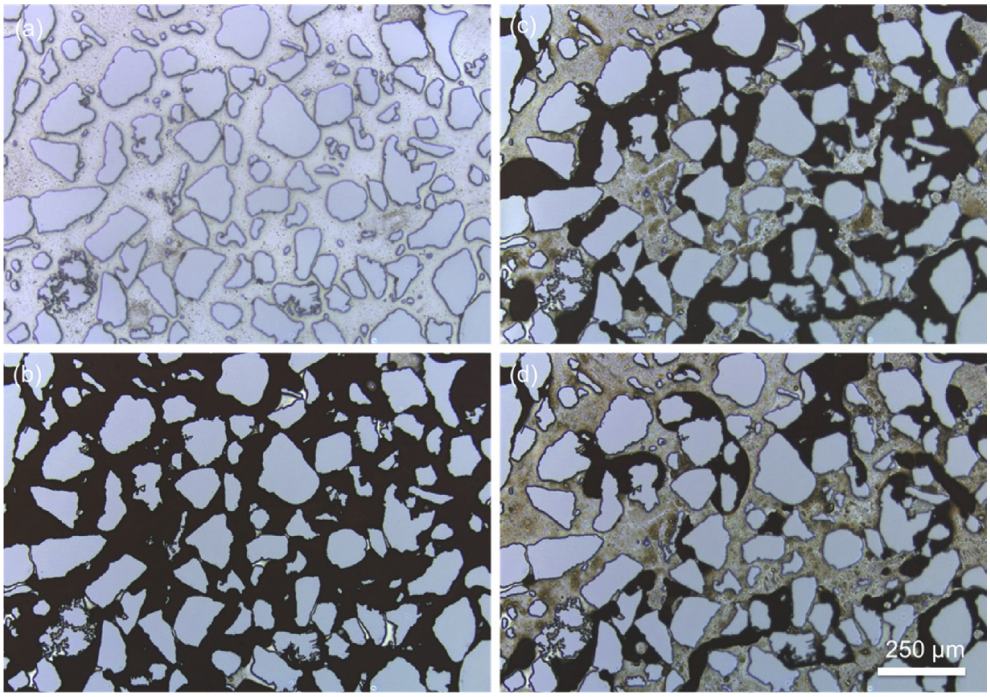

Fig. 4. Direct visualization of pore-level water-oil-clay-silicon phenomena at a fixed pore location near the center of the micromodel. The clay-functionalized pore space that is fully saturated with formation brine (a) is injected with crude oil until residual water saturation is reached and aged to create initial conditions analogous to clastic reservoirs (b). High salinity (10000 ppm brine) waterflooding of the system is performed to standardize the experimental results (c). Low salinity (4000 ppm) brine injection shows decreased pore-level oil saturation, i.e., increased oil recovery and (d) injection of low salinity (4000 ppm) brine injection shows decreased pore-level oil saturation, i.e., increased oil recovery. (For interpretation of the references to colour in this figure legend, the reader is referred to the web version of this article.)

the visual artifacts associated with the adhesion of oil on the pore surface. Mobilization of kaolinite particles in regions with high clay density, however, was observed following the low salinity brine injection, as shown in Fig. 5. Specifically, Fig. 5(a) shows the initial clay particle distribution in formation brine. No clay particle mobilization was observed after the high salinity brine injection, as shown in Fig. 5(b). Clay particle distributions after the low salinity brine injection, however, show that fines mobilization occurred in this case. Comparison between the boxed regions in Fig. 5(b) and (c) shows a deficit of clay particles after the low salinity flood. This correlates well with the mobilization of particles at low salt concentrations in the single-phase experiments.

The minimal local oil mobilization associated with the detachment of clay particles, however, does not correlate well with the significant increase in oil production observed. Because the micromodel was constructed by repeating a single unit of pore geometries across the micromodel, comparison of fluid behavior in repeated pore structures across the micromodel allows for the identification of specific pore geometries that were most sensitive to the experimental conditions. In other words, if a pore geometry was consistently affected by clay mobilization across the micromodel then it was identified as a problematic pore, and similarly, if a pore was consistently affected by oil mobilization across the micromodel then it was deemed an oil mobilization pore. A comparison map identifying the locations of pore-level formation damage was generated at each of the 25 fixed locations across the micromodel by comparing the experimental images before and after the low salinity waterflood. The pores were then matched to the pore geometry map of a single base unit to identify the pores that were most commonly affected by formation damage due to single-phase low salinity waterflooding. A similar treatment of the oil mobilization pores was performed to identify the pores that were most susceptible to increased oil recovery due to low salinity waterflooding. These results are shown in Fig. 6. Specifically, the pores that were consistently affected by formation damage are highlighted in red, while the pores where the brine consistently

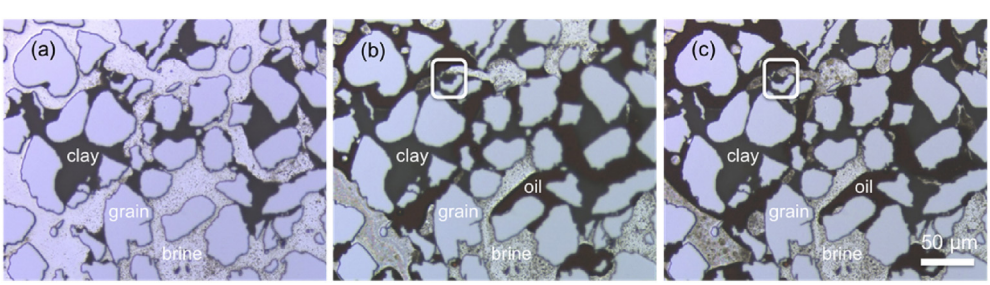

Fig. 5. Mobilization of pore-plugging kaolinite particles as a result of low salinity waterflooding. The initial clay particle distribution is shown for the pore-space saturated in formation brine (a). The deficit of clay particles in the white box after the 4000 ppm low salinity flood (c) in comparison to the clay particles after the 10000 ppm high salinity flood (b) show that similar to the single-phase experiments, clay particles in the two-phase experiments were also sensitive to the salinity of the injection brine.

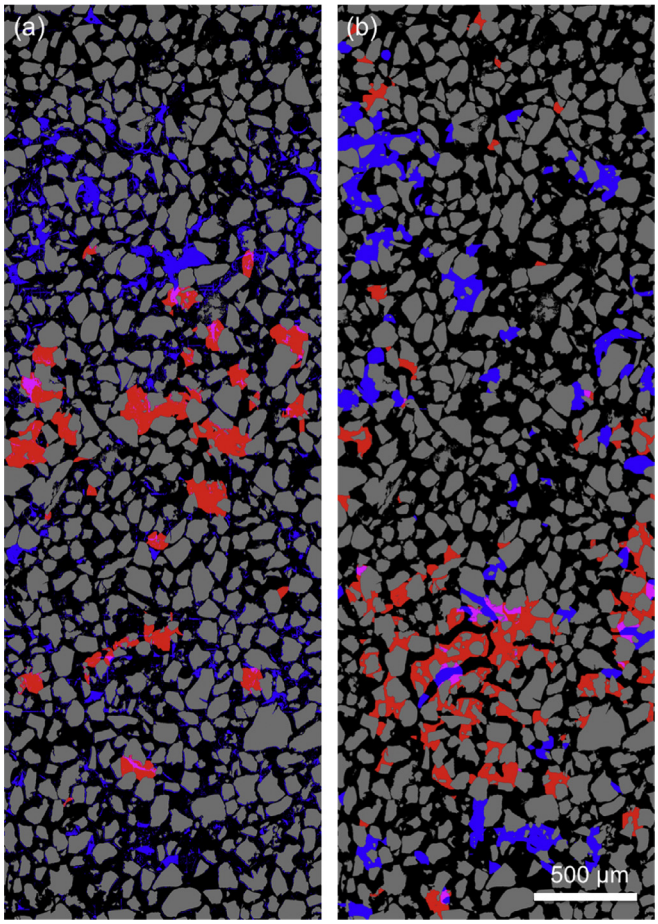

Fig. 6. Comparison of regions affected by clay mobilization (red) and regions of increased oil recovery (blue) compiled on a single base image unit for a kaolinite-functionalized micromodel (a) and a montmorillonite-functionalized micromodel (b). Macroscopic comparisons between the regions that were most susceptible to formation damage with the regions that were most susceptible to oil mobilization of the kaolinite-functionalized system suggest that flow diversion due to formation damage plays a dominant role in low salinity increased oil recovery. (For interpretation of the references to colour in this figure legend, the reader is referred to the web version of this article.)

displaced the oil phase during low salinity waterfloods are highlighted in blue. This analysis was performed for both kaolinite- and montmorillonite-functionalized systems, as shown in Fig. 6(a) and (b), respectively.

Importantly, for the kaolinite-functionalized micromodels, the pores most affected by pore-level formation damage showed minimal increases in oil recovery, and vice versa. Low salinity brine injection most commonly mobilized oil in the smaller pores, i.e., pore radius between roughly 30–80 μm, whereas formation damage most commonly occurred in the larger pores, i.e., pore radius between ~50 μm and 150 μm. These results suggest that the significant redeposition of the mobilized clay particles as pore-plugging structures resulted in drastic blockage of preferential flow paths within the micromodel. As a result, injected brine was diverted to previously unfavorable paths (i.e., pores that were filled with oil) and therefore contribute to the increase in oil recovery observed at concentrations below the critical salt concentration.

Similarly, low salinity waterflooding in montmorillonite-functionalized micromodels showed an 8.5% increase in oil recovery. The pores most affected by clay detachment also showed minimal increases in oil recovery, and vice versa. In this case, however, oil was mobilized in larger pores as a result of low salinity waterflooding, i.e., pore radius between ~80 μm and 130 μm, whereas formation damage most commonly occurred in the smaller pores, i.e., pore radius between ~20 μm and 80 μm. Pore-lining montmorillonite was most commonly found in smaller, low velocity pores at initial conditions and was less prevalent in larger, high velocity flow paths. The mobilization of swollen montmorillonite did not appear to result directly in improved recovery under the conditions studied.

The contrast of results obtained using kaolinite and montmorillonite illustrates, potentially, important effects of the clay type on low salinity waterflooding. Such differences may be related to the nature of nonswelling versus swelling clays and/or the microstructure of clay deposition on pore walls.

4. Conclusion

In this work, pore-level clay particle behavior was visualized directly to delineate the mechanisms contributing to formation damage under low salinity conditions. In contrast to many prior studies, two-phase flow conditions were employed. Montmorillonite- and kaolinite-functionalized pore spaces were subject to low salinity waterfloods. Pressure measurements showed 6-fold reductions in permeability, i.e., significant formation damage in the system accompanying fines mobilization. Drastic swelling-induced fines migration was observed in the montmorillonite-rich system and fines migration was observed in the kaolinite-rich system as brine salinity was reduced below the critical salt concentration. These direct visualization results correspond well to those obtained from previous core-flooding experiments in the literature. Kaolinite detachment and flocculation resulted in (i) the formation of pore-bridging structures across small pores that experienced high velocities and (ii) the redeposition of pore-lining structures on larger pores that experienced intermediate velocities. Two-phase experiments showed increased oil recovery in kaolinite- and montmorillonite-rich rock during low salinity waterflooding where fines mobilization occurred. Mechanisms dictating the increased oil recovery due to low salinity waterflooding were explored by characterizing the pores that were most susceptible to oil mobilization and comparing those to the pores that were most susceptible to formation damage in the kaolinite- and montmorillonite-rich micromodels. Flow diversion from preferential flow paths that became partially blocked with clay to smaller pores containing oil was a major mechanism for increased oil recovery during low salinity waterflooding in kaolinite-rich systems, whereas mobilization of pore-lining swollen montmorillonite did not appear to result directly in improved recovery under the conditions studied.

Acknowledgement

The authors gratefully acknowledge funding from Chevron. Additional funding was provided by the Stanford University Petroleum Research Institute (SUPRI-A) affiliates. The authors thank Dr. C. Soulaine for simulating the flow velocity maps. In addition, the authors gratefully acknowledge the discussions with and help from Dr. C. M. Ross on the structures of clay in natural rock and for designing the micromodel mask.

Appendix A. Supplementary data

Supplementary data related to this article can be found at http://dx.doi.org/10.1016/j.jngse.2016.07.055.

References

Boussour, S., Cissokho, M., Cordier, P., Bertin, H., Hamon, G., 2009. Oil recovery by low salinity brine injection: laboratory results outcrop and reservoir cores. In: Proceedings – SPE Annual Technical Conference and Exhibition, vol. 3, pp. 1595–1606, 2005.

Buchgraber, M., Al-Dossary, M., Ross, C.M., Kovscek, Anthony R., 2012a. Creation of a dual-porosity micromodel for pore-level visualization of multiphase flow. J. Pet. Sci. Eng. 86–87. http://dx.doi.org/10.1016/j.petrol.2012.03.012 (May). Elsevier B.V.: 27–38.

Buchgraber, M., Kovscek, A.R., Castanier, L.M., 2012b. A study of microscale gas trapping using etched silicon micromodels. Transp. Porous Media 95 (3), 647–668. http://dx.doi.org/10.1007/s11242-012-0067-0.

Hadia, Nanji, Lehne, Håvard Heldal, Kumar, Kanwar G., Selboe, Kristoffer, Stensen, Jan Åge, Torsæter, Ole, Norwegian U Science, and Technology Ntnu, 2011. Laboratory investigation of low salinity waterflooding on reservoir rock samples from the frøy field. In: Society of Petroleum Engineers (Ed.), SPE Middle East Oil and Gas Show and Conference.

Hussain, F., South, New, Zeinijahromi, A., Bedrikovetsky, P., Badalyan, A., Carageorgos, T., 2014. Enhanced Oil Recovery through Low Salinity Fines-assisted Waterflooding: Laboratory and Mathematical Modelling Physics Mechanisms of Fines Mobilization, Permeability Decline and. SPE. SPE – 171525 – MS.

Khilar, K.C., Fogler, H.S., 1984. The existence of a critical salt concentration for particle release. J. Colloid Interface Sci. 101 (I), 214–224.

Kia, S.F., Fogler, H.S., Reed, M.G., 1987. Effect of Salt Composition on Clay Release in Berea Sandstones. SPE. SPE 16254.

Lager, Arnaud, Webb, K.J., Black, C.J.J., Singleton, M., Sorbie, K.S., 2008. Low salinity oil recovery – an experimental investigation. Petrophysics 49 (1), 28–35.

Lemon, Phillip Edward, Zeinijahromi, Abbas, Bedrikovetsky, Pavel G., Shahin, Ibrahim, 2011. Effects of injected water chemistry on waterflood sweep efficiency via induced fines migration. In: SPE International Symposium on Oilfield Chemistry. Society of Petroleum Engineers.

Lever, A., Dawe, R.A., 1984. "Water sensitivity and migration of fines in the Hopeman sandstone. J. Pet. Geol. 7 (1), 97–108. http://dx.doi.org/10.1111/j.1747-5457.1984.tb00165.x.

Mcguire, P.L.L., Chatham, J.R.R., Paskvan, F.K.K., Sommer, D.M.M., Carini, F.H.H., B P Exploration, 2005. Low salinity oil recovery: an exciting new EOR opportunity for Alaska's North slope. In: SPE Western Regional Meeting, pp. 1–15. http://dx.doi.org/10.2118/93903-MS.

Mohan, K.Krishna, Ravimadhav, N. Vaidya, Marion, G. Reed, Fogler, H.Scott, 1993. Water sensitivity of Sandstones containing swelling and non-swelling clays. Colloids Surfaces A Physicochem. Eng. Aspects 73, 237–254. http://dx.doi.org/10.1016/0927-7757(93)80019-B.

Peng, Jing, 2009. Heavy-oil Solution Gas Drive and Fracture Reconsolidation of Diatomite during Thermal Operations. Stanford University.

Roman, Sophie, Soulaine, Cyprien, AlSaud, Moataz Abu, Kovscek, Anthony, Tchelepi, Hamdi, 2015. Particle velocimetry analysis of immiscible two-phase flow in micromodels. Adv. Water Resour.

Schembre, J.M., Kovscek, A.R., 2005. Mechanism of formation damage at elevated temperature. J. Energy Resour. Technol. 127 (3), 171. http://dx.doi.org/10.1115/1.1924398.

Schembre, J.M., Kovscek, Anthony R., 2004. Thermally induced fines mobilization: its relationship to wettability and formation damage. In: SPE International Thermal Operations and Heavy Oil Symposium. Society of Petroleum Engineers, Bakersfield, CA, pp. 1–16.

Sinton, David, 2014. Energy: the microfluidic frontier. Lab. Chip 14 (17), 3127–3134. http://dx.doi.org/10.1039/c4lc00267a.

Skrettingland, K., Holt, T., Tweheyo, M.T., Skjevrak, I., 2011. Snorre Low-salinity-water Injection — Coreflooding Experiments and Single-well Field Pilot. SPE Reservoir Evaluation and Engineering, pp. 182–192. http://dx.doi.org/10.2118/129877-PA. April.

Song, Wen, de Haas, Thomas W., Fadaei, Hossein, Sinton, David, 2014a. Chip-off-the-Old-Rock: the study of reservoir-relevant geological processes with real-rock micromodels. Lab. Chip 14 (22), 4382–4390. http://dx.doi.org/10.1039/C4LC00608A. The Royal Society of Chemistry.

Song, Wen, Fadaei, Hossein, Sinton, David, 2014b. Determination of dew point conditions for CO2 with impurities using microfluidics. Environ. Sci. Technol. 48, 3567–3574.

Song, Wen, Kovscek, Anthony R., 2015. Functionalization of micromodels with kaolinite for investigation of low salinity oil-recovery processes. Lab. Chip 15, 3314–3325. http://dx.doi.org/10.1039/C5LC00544B. Royal Society of Chemistry.

Soulaine, Cyprien, 2016. Personal Communication.

Tang, Guo-Qing, Morrow, Norman R., 1999. Influence of brine composition and fines migration on crude oil/brine/rock interactions and oil recovery. J. Pet. Sci. Eng. 24, 99–111.

Zeinijahromi, Abbas, Al-Jassasi, Hammam, Begg, Steve, Bedrikovetski, Pavel, 2015. Improving sweep efficiency of edge-water drive reservoirs using induced formation damage. J. Pet. Sci. Eng. 130, 123–129. http://dx.doi.org/10.1016/j.petrol.2015.04.008. Elsevier.